Available online at www.sciencedirect.com
SCIENCE DIRECT®
Surface Science 590 (2005) L247–L252
SURFACE SCIENCE
www.elsevier.com/locate/susc

Surface Science Letters

Strong lateral growth and crystallization via two-dimensional allotropic transformation of semi-metal Bi film

T. Nagao [a,*], S. Yaginuma [a], M. Saito [b], T. Kogure [c], J.T. Sadowski [a], T. Ohno [b], S. Hasegawa [d], T. Sakurai [a]

[a] *Institute for Materials Research, Tohoku University, Sendai 980-8577, Japan*
[b] *National Institute for Materials Science, Tsukuba 305-0047, Japan*
[c] *Department of Earth & Planetary Science, University of Tokyo, Tokyo 113-0033, Japan*
[d] *Department of Physics, University of Tokyo, Tokyo 113-0033, Japan*

Received 5 April 2005; accepted for publication 3 June 2005
Available online 11 July 2005

Abstract

Two-dimensional (2D) nano-objects, such as metallic nanofilms are the most fundamental building blocks for nano-electronics devices. However, the fabrication of highly ordered nanofilms has been difficult because of well known Stranski–Krastanov growth, which results in rough growth front and high density grains. Here we report on the unusual high-quality film growth of Bi on a Si surface with atomic-level surface/interface smoothness and high film crystallinity. The formation of a newly discovered 2D allotrope was clarified to initiate its strong 2D growth. Above several-monolayer thickness, the 2D allotrope transforms into a single-crystalline film with bulk-like layered structure. Our study unveils the atomistic growth process of nano-sized Bi, and the obtained knowledge here will be generally applicable for the fabrication of various nano-devices using this intriguing material that shows rich thermal, magnetic, electronic properties in nanometer scale.

Keywords: Bi; Epitaxial growth; Structural transformation; LEED; STM

Heteroepitaxial growth of metal overlayers on semi-conductor surfaces is governed by a variety of factors which arise from the differences in lattice constants, chemical bonding (metallic versus covalent), and kinetics of the growth. It is widely accepted that metal overlayers on semi-conductor surfaces always grow in 3D mode after completion

* Corresponding author. Tel./fax: +81298604746.
E-mail address: nagao.tadaaki@nims.go.jp (T. Nagao).

0039-6028/$ - see front matter © 2005 Elsevier B.V. All rights reserved.
doi:10.1016/j.susc.2005.06.004

of the first wetting layer and that island interconnection is observed well above a few dozens of monolayers [1,2]. This growth, Stranski–Krastanov (SK) growth, has been the most severe drawback for fabricating atomically thin high-quality conductive overlayers compatible with modern nanoelectronics as well as for exploring the atomic scale 2D transport properties undisturbed by the presence of defects [1,3]. By modifying the kinetics of the film, for example, by low-temperature (LT) deposition or by surfactant mediated growth, well connected relatively flat film can be fabricated. However, such films always contain unwanted defects such as surfactant impurity atoms or high density of grain boundaries [2,3].

In this letter, we report on the unusual 2D growth of ultrathin Bi film on the Si surface, which exhibits striking difference from the commonly observed SK growth for metallic overlayers. Bi has been one of the most extensively studied materials next to Si and Ge for the past three quarters of century. Recently, there is renewed growing interest in its device properties in nanometer scale because of its strong size/interface effects in electronic/magnetic properties [4–6]. Also, it has attracted strong interest most recently because of its unusual structural and vibrational properties originated from its unique intermediate bonding character between metallic and covalent [7–9]. However, even the most basic understanding on the atomistic growth process of Bi nanostructures has been lacking so far. We have revealed the nanomorphology evolution during the growth of ultrathin Bi film by using scanning tunneling microscopy (STM), reflection high-energy electron diffraction (RHEED), and in situ conductance measurements. The unusually strong 2D film growth is initiated with the formation of a newly discovered 2D allotrope and the following structural transformation into the bulk-like (0 0 1) phase, which yields two-step conductance shoot up as a function of film thickness. Both phases have unique 2D layered structures and thus the strong lateral growth is motivated. The crystallinity of the surface, interface, as well as internal portion of the film was revealed to be excellently high, which was evidenced by the spot-profile-analyzing low-energy electron diffraction (SPA-LEED), cross-sectional transmission electron micrograph (XTEM), and electron backscattering pattern (EBSP) experiments.

Bismuth ultrathin films were grown in ultrahigh vacuum (UHV) and characterized in situ using RHEED and STM. In situ conductance measurement and SPA-LEED with momentum resolution better than 0.005 Å^{-1} were performed in a separate UHV system. Bi was evaporated from an alumina-coated tungsten basket on a clean Si(1 1 1)-7×7 surface (on an n-type $\sim$1 Ω cm wafer). All the experiments were performed under $<1\times10^{-10}$ Torr condition at room temperature (RT). For indexing the crystal face of bulk Bi, we adopt here the simplest hexagonal coordinates; $|\mathbf{a}| = |\mathbf{b}| = 4.54$ Å and trigonal axis $|\mathbf{c}| = 11.8$ Å. Bi deposition rate was 0.43 ML/min, calibrated by ex situ Rutherford backscattering experiments within 6% errors. Here, we define 1 ML as the density of Bi atoms in a pseudocubic Bi{0 1 2} plane (9.28×10^{14} atoms/cm^2) which has the highest atom density.

Fig. 1 shows a series of STM pictures and the film conductance taken as a function of Bi thickness. The conductance of the Bi film is derived by subtracting the conductance of the initial clean substrate from the measured total conductance during the growth. The film growth can be classified into five stages (i)–(v). In stage (i), Bi atoms are adsorbed randomly on the Si(1 1 1)-7×7 surface to form a uniform wetting layer. In stage (ii), islands start to nucleate as expected for the conventional SK growth commonly observed for the metal-on-semi-conductor film growth. In stage (iii), however, the islands grow only laterally and begin to interconnect each other. After the interconnection (stage (iv)), the film morphology becomes remarkably smooth, and then, film crystallinity becomes higher as can be seen from the well defined step direction of the film surface (stage (v)).

Conductance change in stages (i) and (ii) is negligibly small indicating that the wetting layer nor the islands do not form substantial current path. At stage (iii), the conductance starts to increase indicating the formation of macroscopic current path through the film. This conductance increase is consistent with the island interconnection observed in STM and indicates the metallic nature

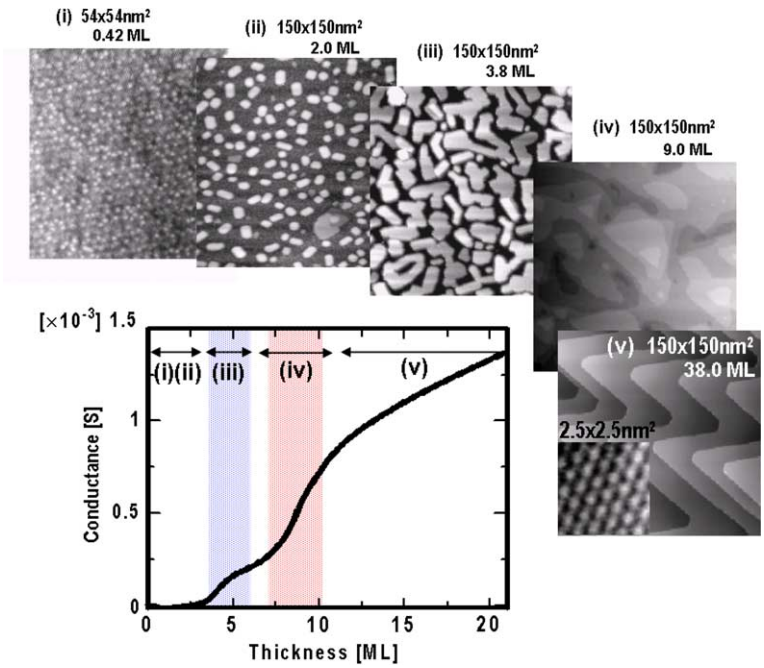

Fig. 1. (color online) Evolution of surface morphology observed by STM and dc conductance of the film, measured as a function of Bi film thickness. In stage (iii), the conductance increases due to the island percolation. The following conductance increase in stage (iv), cannot be understood solely by the surface morphology.

of the islands. In stage (iv), we observed another unexpected rapid increase in the conductance. In this coverage range, there is no remarkable morphology change such as seen in stage (iii). We can recognize the change in the surface step morphology which transforms from meandering ones to straight ones which may be the indication of structural transformation of the Bi film.

To extract more precise crystallographic information of the film, we performed electron diffraction experiments during the growth. Fig. 2 shows SPA-LEED 2D patterns (left) and 1D profiles (right) taken at thicknesses of 4.7 ML (stage (iii)) and 16.8 ML (stage (v)). Four different profiles labeled (a)–(d) in the right-hand side correspond to the line scans of (a)–(d) in the 2D patterns in the left-hand side. In the 2D pattern taken at 4.7 ML (upper left), texture ring $\mathbf{R}_{\mathrm{Bi}}$ is observed. The radius of this ring is 1.902 ± 0.002 Å^{-1}, located slightly outside the (10)-type spots of the substrate Si(111). This can be seen clearly by comparing the 1D scan data (a) and (b) which are taken in slightly different directions. The value of the ring radius precisely matches to the one expected for the texture ring from the {012} oriented Bi islands. So, the film orientation is most possibly the {012} orientation.

At larger thickness, the ring $\mathbf{R}_{\mathrm{Bi}}$ becomes weaker and sharp spots with threefold symmetry appear. The (00) spot and one of the (10)-type spots of this Bi overlayer are shown in the second 2D scan taken at 16.8 ML (middle left). For comparison, 2D pattern for the clean Si(111)-7×7 surface before Bi deposition is also shown in (d) (lower left). Distance between the $(00)_{\mathrm{Bi}}$ and $(01)_{\mathrm{Bi}}$ spots is 1.620 ± 0.002 Å^{-1} which is close to the value expected for the Bi(001) surface, and its threefold symmetry also agrees with Bi(001). As can be seen from the comparison between (c) and (d), it should be noted that $(10)_{\mathrm{Bi}}$ spot locates exactly at the position of $(6/7\,0)_{\mathrm{Si}}$ spot of the substrate Si(111)-7×7 surface. This indicates that the Bi(001) film grows commensurately on the Si(111)-7×7 substrate with a relation of

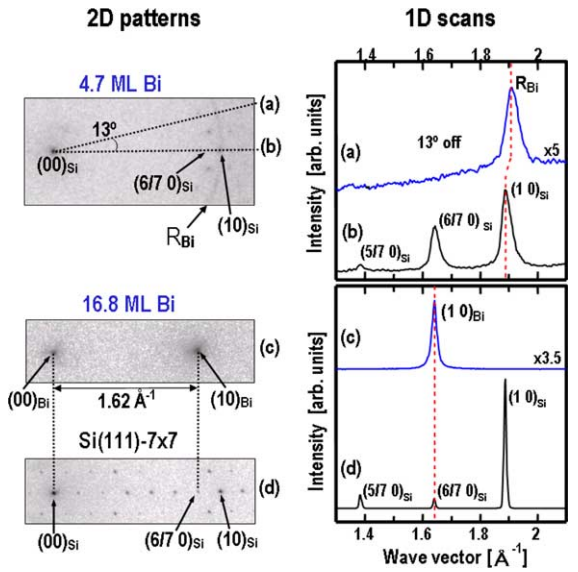

Fig. 2. (color online) SPA-LEED 2D pattern (left column) and 1D profiles (right column) taken at thicknesses of 4.7 ML (stage (iii)) and 16.8 ML (stage (v)). Four different 1D scans labeled (a)–(d) in the right-hand side correspond to the line scans with the same labels in the left column. In the 2D pattern taken at 4.7 ML (upper left), texture ring $\mathbf{R}_{\mathrm{Bi}}$ is observed. The radius of the ring $\mathbf{R}_{\mathrm{Bi}}$ is 1.902 ± 0.002 Å^{-1}, corresponding to the expected value for the texture ring from the {012} oriented Bi islands. Position of the (01) type spot of the 16.8 ML film locates exactly at the position of (6/70) spot position of the substrate Si(111)-7×7, which indicates the commensurate growth of the Bi(001) film on the Si(111)-7×7 surface.

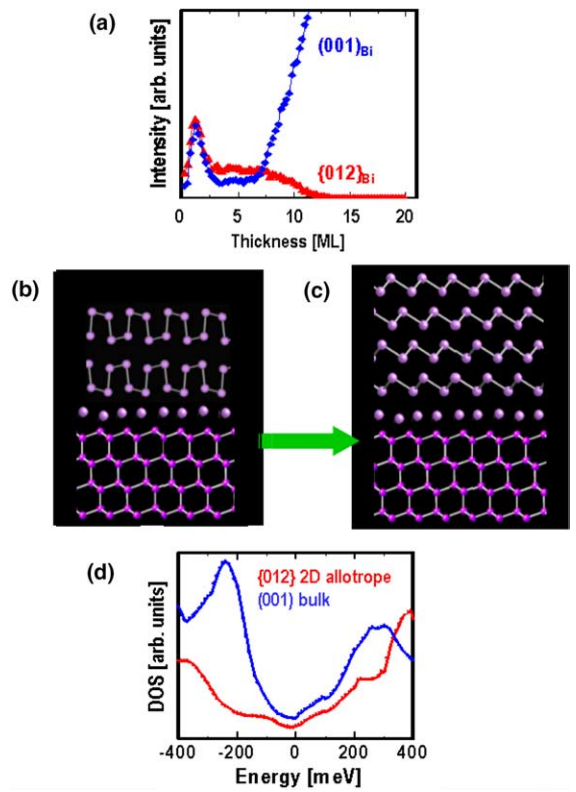

Fig. 3. (color online) (a) Diffraction intensity taken as a function of Bi thickness. Triangles (red) correspond to the diffraction from the {012} grains, and the diamonds (blue) correspond to the bulk-like (001) grains. The (001) phase completely takes over the {012} phase in the thickness range corresponds to stage (iv) in Fig. 1. (b) Schematic illustration of the {012}-like "new 2D allotrope". Unique puckered-layer structure is formed at lower thickness. (c) Bulk-like (001) phase appears at higher thickness. (d) Density of states (DOS) calculated for the new 2D allotrope phase (red) and the bulk phase (blue). DOS of {012}-like 2D allotrope phase is lower compared to that of the (001) phase.

$6|\mathbf{a}_{\mathrm{Bi(f)}}| = 7|\mathbf{a}_{\mathrm{Si}}|$ (which can be called "coincidence lattice" or "magic mismatch" [10]), where $|\mathbf{a}_{\mathrm{Si}}| = 3.84$ Å is a unit cell of the Si(111) plane. The lattice constant of the Bi(001) film is $|\mathbf{a}_{\mathrm{Bi\ film}}| = 4.480 \pm 0.004$ Å, which is compressed by 1.3% from the bulk value in the film parallel direction.

Evolution of the structural transformation from the {012} phase to the (001) phase as a function of thickness was monitored by RHEED spot intensity measurement for different structural components of the film (Fig. 3(a)). The red curve shows the intensity of the ring $\mathbf{R}_{\mathrm{Bi}}$ which corresponds to the {012} phase and the blue curve shows the intensity of the (11)-type spot from the (001) phase. At around 1.3 ML, both curves show sharp maxima due to the increased reflectivity of the surface possibly associated with the increased smoothness of the wetting layer. At around 7 ML, dramatic increase in the (001) intensity and simultaneous decrease in the {012} intensity take place, indicating that the film undergoes a structural transformation from the {012} phase to the (001) phase. This transformation occurs in stage (iv) in Fig. 1 where the second rapid increase in conductance takes place, thus indicating this conductance increase is strongly correlated to the transformation from the {012} to (001) phase. A part of the conductance increase is related to the crystallographic structure change.

Rest of the contribution to the conductance increase is ascribed to the reduction in the grain boundary scattering due to the crystallinity change from textured to single-crystalline film. Our Si sample has 1.4 kΩ resistance and its size is 8 mm × 8 mm × 0.4 mm and the total resistance at 22 ML (70 Å thick) was 0.445 kΩ, thus the resistivity of the film at 22 ML can be roughly estimated as 4.5×10^{-4} Ω cm. This value is about four times higher than the bulk value. In the present experiment, we do not quantify the contributions from the surface-state transport and interface carrier scattering. But, we expect that the contribution from the surface-state will be rather significant because the presence of dangling bonds should make the surface highly metallic from semimetallic.

The unusual structural transformation from the {012} to (001) phase is understood by our theoretical simulation based on first principle total energy calculation. Surprisingly, we found that the low-thickness {012} phase actually takes a very unique 2D structure analogous to that of bulk black phosphorus (Fig. 3(b)). The film stabilizes by taking a so-called "puckered-layer structure" while the unit cell size and the layer spacing of this phase remain identical to those of bulk {012} structure. This new structure is a kind of teratoid structure which is never found in any other one-component bulk crystal except for phosphorus [7,9]. Therefore, this unusual 2D layered structure can be called as "a new 2D allotrope" only stabilized in ultrathin regime. The stability of this 2D allotrope is higher by about 40 meV/atom compared with that of the (001) bilayer at 2 ML. Since black phosphorus is semi-conductor, this new Bi 2D allotrope was also expected to be semi-conductor. However, our conductance measurement indicated that this 2D allotrope is metallic. This fact strongly suggests the presence of the metallic surface/interface states on this 2D allotrope, and actually our theoretical result shows the presence of surface density of states near Fermi level. Theoretical comparison between the metallicity of the 2D allotrope and the bulk-like (001) phase has indicated that the density of states at the Fermi level is higher for the Bi(001) face. This can be one of the strongest reasons for the observed conductance increase in stage (iv), as discussed above.

Our calculation clarified that the {012}-like 2D allotrope becomes substantially unstable with the increase of thickness and finally converts into the (001) phase. The reason for the stability conversion of the two phases is explained as follows. In a hexagonal (001) phase, the surface Bi atoms lose three second nearest (2NN) bonds. On the other hand, in the {012}-like allotrope phase (Fig. 3(b)), the surface Bi atom loses only one 2NN bond. Therefore the latter is more stable than the former at small thickness. As the thickness increases, one can expect that the surface effect becomes less dominant and the cohesive energy swiftly approaches to the bulk value. This holds true for the case of the bulk-like (001) phase. On the other hand, for the case of the {012}-like 2D allotrope, its cohesive energy cannot approach to the bulk value even at larger thickness because of the presence of strain due to buckling in the puckered-layer structure (see Fig. 3(b)). Therefore the stabilization of the {012}-like phase is only possible at small thickness.

Experimentally, the structural transformation proceeds very rapidly once it started as seen in the blow-up in the spot intensity of the (001) component (Fig. 3(a)). The spot intensity rapidly increases and then slows down above 15 ML. This is because the growth of the (001) area releases the heat and continuously triggers the successive conversion of the surrounding {012} texture grains into the crystalline (001) film. At the growth front, the structural conversion takes place easily even at room temperature (possibly with rather small energy barrier) since this transformation only involves the conversion of the bond orientation and does not require much atom diffusion.

Because of the characteristic layered structures of these two phases, the strong 2D growth, i.e., bilayer-by-bilayer growth takes place in both phases. The role of the low-thickness {012}-like 2D allotrope is to achieve perfect wetting, or perfect covering of the substrate by the lateral growth and the following interconnection of tabular islands. After this perfect wetting, at around 7 ML, *allotropic transformation* into the more

stable bulk-like (0 0 1) phase takes place, and further stabilizes the film by the elimination of grain boundary stain as well as the reduction in the interface energy via commensurate growth. Essential part of the driving force of this unique growth originates from the intermediate bonding character of Bi. That is, the average coordination number is reduced at small thickness and therefore the shift from the metallic side to the covalent side in the chemical bonds takes place, which is an intriguing analogy to the pressure effect in bulk group V semi-metals. As a result, covalent like bonds form layered structure and thus the observed strong 2D growth, which is in striking difference from the conventional SK growth takes place.

We also studied the internal crystal structure of the film by EBSP and XTEM. The observed EBSP pattern (Fig. 4(a) and (b)), indicates high crystallinity and the epitaxial relationship across the macroscopic area of our sample (3 mm × 8 mm). By comparing the simulated Kikuchi pattern (Fig. 4(a′) and (b′)) with the experimental data (Fig. 4(a) and (b)), crystal structure of the Bi film was confirmed to be identical to that of the rhombohedral A7 structure of bulk Bi. The [1 0 0] axis of the Bi(0 0 1) overlayer is aligned to the $[0\,\bar{1}\,1]$ axis of the Si substrate. High crystallinity is also confirmed by the XTEM observation. Fig. 4(c) is the XTEM image viewed from the $[0\,\bar{1}\,1]$ direction of the Si substrate. Excellent long-range ordering in the film as well as abrupt vacuum/Bi and Bi/Si interfaces were clarified. Sharpness of the Bi/Si interface is more clearly shown in the magnified picture of Fig. 4(c′). Even higher crystallinity is achieved when the film is annealed in vacuo above 350 K [11].

Increasing importance and interest exists in the electronic/magnetic device properties of Bi-based low-dimensional nanostructures. Our study has elucidated for the first time the evolution of nanomorphology and crystallinity of ultrathin film of Bi which is the most important as well as the most prototypical structure among various Bi nanostructures. The knowledge obtained here can provide us noble information for further tailoring various nanometer-scale device structures by utilizing its strong size effects and interface effects of this intriguing material [12].

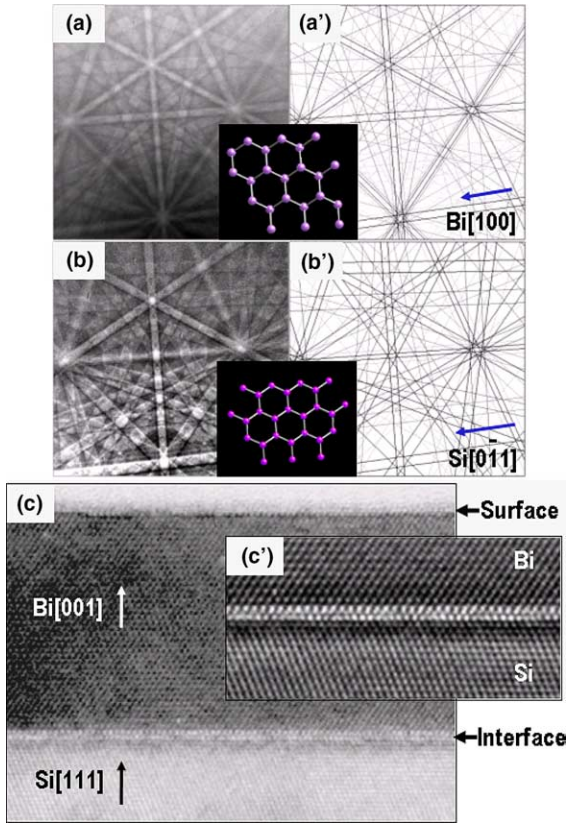

Fig. 4. (color online) (a) Electron backscattering pattern (EBSP) form the Bi(0 0 1) overlayer. (b) EBSP from the clean Si(1 1 1) surface without Bi overlayer. (a′) Simulated Kikuchi pattern for Bi(0 0 1) film. (b′) Simulated Kikuchi pattern for the Si(1 1 1) surface. (c) Cross-sectional transmission electron micrograph (XTEM) of the Bi(0 0 1)/Si(1 1 1) interface viewed from the $[0\,\bar{1}\,1]$ direction of the Si substrate. No filtering was processed. (c′) Magnified image near the Bi/Si interface. Fast Fourier transform filtering was processed.

References

[1] M. Henzler et al., Surf. Sci. 438 (1999) 178.
[2] A. Koch et al., Europhys. Lett. 21 (2) (1993) 123.
[3] F. Moresco, M. Rocca, T. Hildebrandt, M. Henzler, Surf. Sci. 463 (2000) 22.
[4] F.Y. Yang et al., Science 284 (1999) 1335.
[5] C.A. Hoffman et al., Phys. Rev. B 48 (1993) 11431.
[6] Y.M. Koroteev et al., Phys. Rev. Lett. 93 (2004) 046403.
[7] H. Iwasaki, T. Kikegawa, Acta Cryst. B 53 (1997) 353.
[8] K. Sokolowski Tinten et al., Nature 422 (2003) 287.
[9] T. Nagao et al., Phys. Rev. Lett. 93 (2004) 105501.
[10] J. Tolle et al., Appl. Phys. Lett. 82 (2003) 2398.
[11] S. Yaginuma et al., Surf. Sci. Lett. 547 (2003) L877.
[12] J.T Sadowski et al., Appl. Phys. Lett. 86 (2005) 073109.